Use of collocation methods under inclusion of a priori information in acoustic pyrometry

Helmut Sielschott[1] Willy Derichs[2]
University of Münster RWE Energie AG

Published in:

Process Tomography – 95 Implementation for Industrial Processes (Manchester: UMIST)
Editors: M.S. Beck, B.S. Hoyle, M.A. Morris, R.C. Waterfall, R.A. Williams, pages 110–117
ISBN 0 9523165 2 8
(Proc. European Concerted Action on Process Tomography, Bergen, Norway, 6-8 April, 1995)

[1]Institut für Numerische und instrumentelle Mathematik, Einsteinstr. 62, D-48149 Münster. E-mail: helmut.sielschott@uni-muenster.de
[2]Kraftwerk Niederaußem, Abt. KF-F, Postfach 1461, D-50104 Bergheim

Use of collocation methods under inclusion of a priori information in acoustic pyrometry

H. Sielschott*, W. Derichs+

**Institut für Numerische und instrumentelle Mathematik, Einsteinstraße 62, D-48149 Münster, E-mail: helmut.sielschott@uni-muenster.de*
+*RWE Energie AG, Abt. KF-F, Kraftwerk Niederaußem, Postfach 1461, D-50104 Bergheim*

ABSTRACT: Acoustic pyrometry is a tomographic technique for measuring the temperature distribution of gas. As the number of lines is very small, collocation methods with smooth ansatzfunctions lead to a sufficiently fast reconstruction algorithm. The resulting system of linear equations is solved using the method of Tikhonov-Phillips. Two simple but effective methods for including a priori information are presented and applied to artificial and to measured data.

KEYWORDS: *few-data-tomography, a priori information, acoustic pyrometry, collocation methods.*

1. INTRODUCTION

The aim is to recover the temperature distribution $f(x)$ in a horizontal layer in a combustion chamber of a brown coal fired power station. Further publications on this application are [1], [2], [3].

Eight transceivers, each consisting of a microphone and a kind of loudspeaker, have been attached to the walls of the furnace. The scanning geometry with 24 lines shown

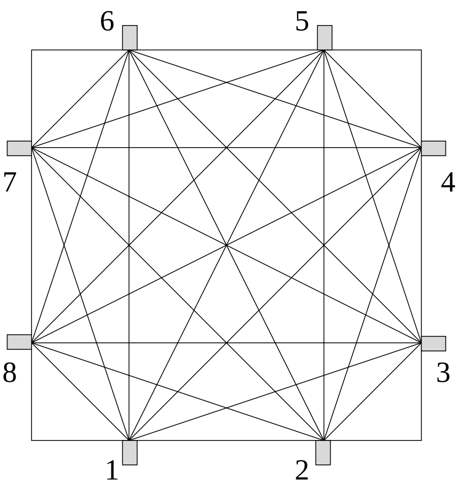

Fig 1: Scanning geometry

in Fig. 1 is obtained. Measuring the propagation time of sound, we can compute the mean temperature on each line. There are several kinds of approximation errors in this procedure, e.g. the relation between temperature and sound velocity is not linear. However, approximation errors are clearly dominated by errors in measurement. Because of bending–phenomena, measurements taken between transceivers on the same wall cannot be used.

2. A COLLOCATION METHOD

As we know the mean temperature on each line $L_1, ..., L_{24}$, the values

$$g_l := \int_{L_l} f(x)\, ds, \qquad x \in \mathbb{R}^2, \quad l = 1, \ldots, 24 \tag{1}$$

are available. The simple idea of a collocation method is to build up the reconstruction in the form ($n \in \mathbb{N}$)

$$f(x) = \sum_{k=1}^{n} \xi_k\, \varphi_k(x) \quad . \tag{2}$$

To get a system of equations for the coefficients ξ_k, we combine (1) and (2):

$$\begin{aligned} g_l &\overset{!}{=} \int_{L_l} \sum_{k=1}^{n} \xi_k\, \varphi_k(x)\, ds = \sum_{k=1}^{n} \xi_k \underbrace{\int_{L_l} \varphi_k(x)\, ds}_{=:a_{lk}} \quad , \quad l = 1, \ldots, 24 \\ \leadsto g_l &= \sum_{k=1}^{n} a_{lk}\, \xi_k \qquad , \quad l = 1, \ldots, 24 \end{aligned}$$

With the definitions

$$\begin{aligned} A &:= (a_{lk})_{\substack{l=1,\ldots,24 \\ k=1,\ldots,n}} && \in \mathbb{R}^{24\times n} \\ g &:= (g_1, ..., g_{24})^t && \in \mathbb{R}^{24} \\ \xi &:= (\xi_1, ..., \xi_n)^t && \in \mathbb{R}^{n} \end{aligned}$$

we arrive at the problem to find a vector ξ which solves

$$A\xi = g \quad . \tag{3}$$

As A is ill-conditioned in these applications, the method of Tikhonov-Phillips is used to get a good approximation to the “solution” of equation (3). So we are looking for a minimizer of

$$||A\xi - g||^2 + \gamma ||\xi||^2 \quad .$$

The real number γ serves as a parameter, controlling the regularisation. Using the singular value decomposition of A, we can calculate this minimizer with a direct method (see [4, chapter IV.1]).

The ansatzfunctions φ_k are not described yet. The reconstruction region is divided into 10×10 pixels and $\varphi_k(x) = e^{-\lambda|x-x_k|^2}$ is chosen, where x_k, $k = 1, ..., 100$ are the midpoints of the pixels, and $n = 100$. With this scanning geometry, a good choice for λ is $\lambda = 8.0$, if the reconstruction region is transformed into a square with sidelength 1. As the number of ansatzfunctions is much higher than the number of lines, you cannot see the special characteristics of the chosen ansatzfunctions in the reconstructions. A good choice of ansatzfunctions is achieved, if all details of the functions can be seen from their tomography data. Nevertheless it must be possible to build up details of the required resolution from the ansatzfunctions.

In [5] the method of Tikhonov-Phillips is introduced in a more general way. For their application the authors are looking for a minimizer of

$$||A\xi - g||^2 + \gamma||D\xi||^2$$

with a properly chosen diagonal matrix D. The elements of D can be chosen in such a way that high-frequency ansatzfunctions are weighted different to low-frequency ones. This is not necessary for ansatzfunctions like $\varphi_k(x) = e^{-\lambda|x-x_k|^2}$ as these are only shifted versions of the same function, so $D = I$ is a good choice here. A more detailed investigation on the solution method shows that even when using $D = I$ the high frequency parts of the reconstructions are less emphasized than the low frequency ones (see [6]).

In this application, computing time is no problem. For applications with a higher number of lines the functions proposed in [7] may be a better choice as they are "numerically compact supported".

Using this technique, we can find reconstructions of the temperature distributions that fulfill the data as good as required (depending on γ). We are not looking for an exact solution, as the reconstruction problem is ill-posed and we face noisy data.

Having only 24 lines, our reconstructions cannot have more degrees of freedom than 24. In this method, all reconstructions are in a 24-dimensional subspace of span(φ_k). As we are using the method of Tikhonov-Phillips, the reconstructions are in some sense as smooth as possible under the condition to fulfill the data. However, the real temperature distribution is less smooth and there is no information about the difference between the reconstruction and the real situation in the measured data. So we have to use further knowledge to get reconstructions of value for the operators.

Two methods, both basing on the same idea, are proposed here.

3. USE OF STARTING PICTURES

The idea to use a starting picture is taken from [8]. The engineers have quite a good knowledge of the general temperature situation in the furnace. These information come from other measurement techniques like suction pyrometry and radiation pyrometry and from theoretical considerations.

Let $h(x)$ be a realistic temperature distribution and $h_l := \int_{L_l} h(x)ds$. The reconstruction f is build up in the form

$$f(x) = \kappa h(x) + u(x) \quad . \tag{4}$$

Here $\kappa \in \mathbb{R}$ is chosen in order to make $\kappa h(x)$ fulfill the measured data as good as possible in the sense that

$$\sum_{i=1}^{24} (\kappa h_i - g_i)^2$$

is minimized. Looking for the minimum by differentiation with respect to κ leads to

$$\kappa = \left(\sum_{i=1}^{24} h_i g_i\right) \cdot \left(\sum_{i=1}^{24} h_i^2\right)^{-1} \quad .$$

Next $u(x)$ is computed as a reconstruction from the line integrals

$$u_l := g_l - \kappa h_l \quad , \quad l = 1, ..., 24$$

using the collocation method proposed above.

The real number κ is introduced because only *structures* are to be build in by the starting picture. The influence of the starting picture should be independent from its absolute values. This is important when for example the starting up of a furnace is observed.

The use of a starting picture gives us a reconstruction f which on the one hand shows the structures of $h(x)$ and on the other hand fulfills the measured data as good as required.

4. SMOOTHING IN THE HIGH TEMPERATURE AREA

From measurements via suction pyrometry it is known that the real temperature distribution is rather constant in the hot part of the furnace. However, collocation methods tend to produce non-realistic "peaks". To correct this behaviour we change the reconstructed temperature distribution in order to make it suit to this a priori information and correct it afterwards to arrive at a new reconstruction that also fulfills the data.

Think of $h(x)$ to be a computed reconstruction. Define $M := \max_x h(x) - c$ and

$$\bar{h}(x) := \begin{cases} h(x) & , \text{ if } h(x) \leq M \\ M & , \text{ if } h(x) > M \end{cases} ,$$

where c is a constant equivalent to 50°C for example. This picture $\bar{h}$ perfectly fulfills the a priori information. To include the data we use the final reconstruction

$$f(x) = \bar{h}(x) + u(x)$$

where $u(x)$ is computed using a collocation method in order to make f fulfill the measured data.

This method can be used for many different kinds of a priori information:

1. compute a reconstruction $h(x)$,
2. change it according to the a priori information into a function $\bar{h}(x)$,
3. correct this to fulfill the measured data by computing and adding $u(x)$.

The last two steps can be repeated several times of course, resulting in an iterative method, but it is not recommendable to repeat this procedure more than two or three times, as it usually does not converge. For converging methods see for example [9] and [10]. Apart from this, after a few iterations of this type the reconstruction fulfills the data in a very good way, so we have non-regularised reconstructions and therefore new kinds of artefacts caused by errors in measurement.

5. NUMERICAL RESULTS: ARTIFICIAL DATA

To test the proposed methods we first reconstruct some artificial temperature distributions, so-called "phantoms". Three phantoms are shown in the first row of Fig. 2. The greyscale lies in the interval between 850°C (black) and 1250°C (white). The phantoms are called "asymmetric block profile", "asymmetric complex profile" and "block profile". Below there are reconstructions from tomographic data of the phantoms with different methods. In the left column the used starting pictures are shown.

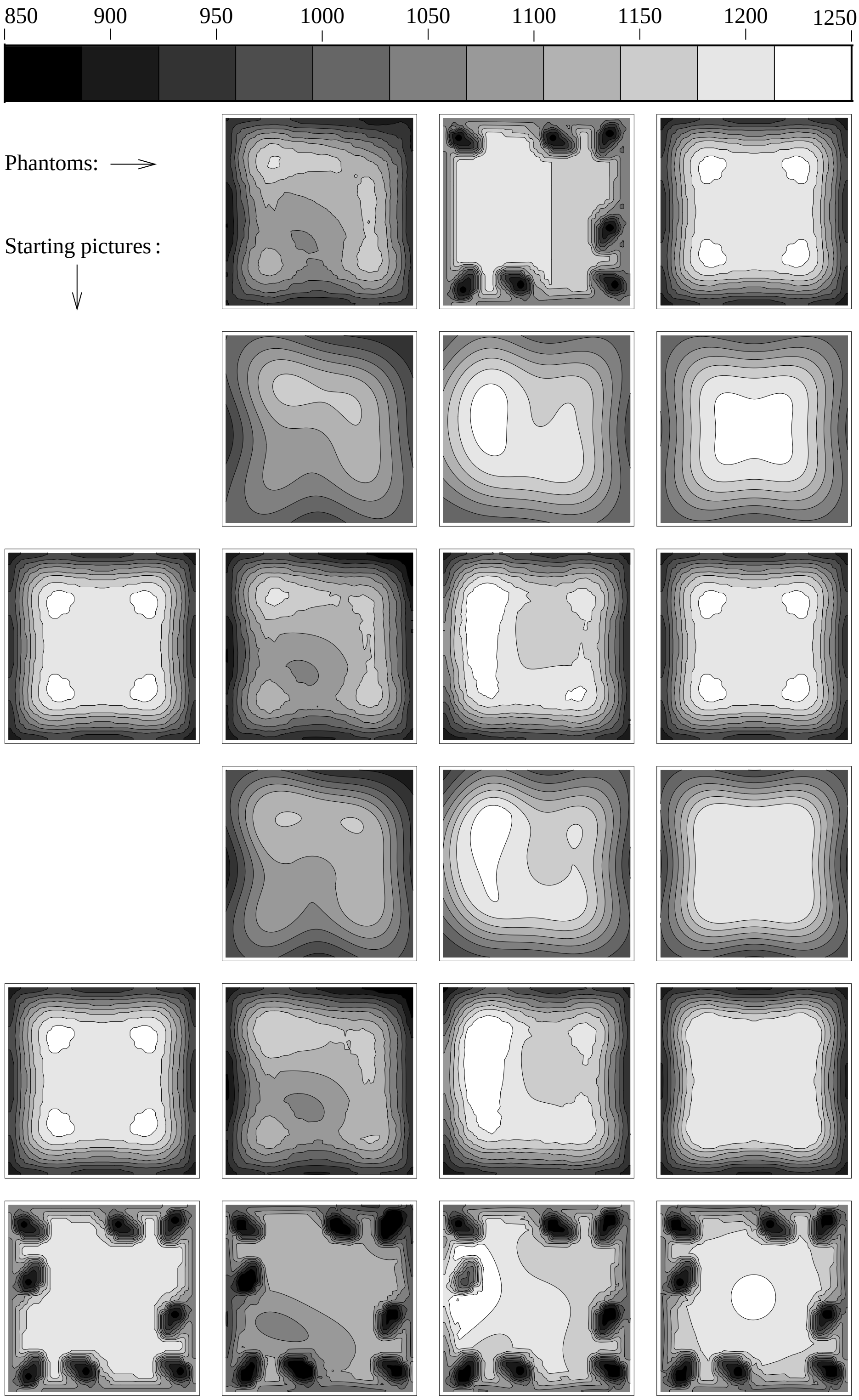

Fig 2: Numerical results using artificial data

Fig. 2 shows the following:

<u>First row:</u>	phantoms
<u>Second row:</u>	reconstructions without a priori information
<u>Third row:</u>	reconstructions with starting picture
<u>Fourth row:</u>	reconstructions with smoothing
<u>Fifth row:</u>	reconstructions with starting picture and smoothing
<u>Sixth row:</u>	reconstructions with detailed starting picture and smoothing

The reconstructions without a priori information (second row) give us rough approximations to the phantoms. Remember that these pictures do fulfill the data, the regularisation parameter γ was chosen in order to reproduce the line integrals with an error of about 1%. Next, the block profile is taken as starting picture (third row). This leads to a perfect "reconstruction" of the block profile itself, of course. However, the reconstructions of the other two phantoms are much better as well, because at the border both of them are similar to the starting picture.

The asymmetric block profile does not suit to the a priori information: "the hot part is rather constant". Applying the smoothing in this case leads away from the phantom (fourth row)! However, the reconstruction of the block profile is getting better although no starting picture is used. Adding a starting picture (fifth row), we get good reconstructions of all phantoms.

The small details in the asymmetric complex phantom, simulating the blow-in of cold air at a level just below the measurement layer turn out to be too small to be found from only 24 line integrals. They can be build in by an appropriate starting picture, of course. This is shown in the last row using a symmetric complex profile. Pay attention to the left part of the reconstruction of the asymmetric complex profile. The collocation method tries to correct the dark spot of the phantom but it cannot produce sufficient small details.

These results indicate that you should only use such a detailed starting picture incase you know for sure that the small details are realistic, as they can not be corrected by the collocation method.

A comprehensive analysis of the results using noisy data and an increased number of transceivers can be found in [6].

6. NUMERICAL RESULTS: MEASURED DATA

It takes about 40 seconds to receive the complete set of 24 line integrals. Two methods for displaying the results are available: during measurements the data of about 7 minutes have been used to get one reconstruction of the average situation in the chamber. To analyse the results subsequently a film can be produced to show the reconstructed temperature distributions of several hours.

To get data for any given point of time the measured line integrals for one path in one direction are approximated by a cubic spline as shown in Fig. 3. Clearly wrong measurements or drop-out times of transceivers are handled by replacing these with linear interpolated values of the "good" measurements in the neighbourhood. To make a film, the splines are evaluated for every thirty seconds for example resulting in a big number of reconstructed pictures which are compressed into an mpeg-movie afterwards.

Fig. 4 shows a reconstruction from measured data given in [11]. It is plotted in the way the reconstructions are presented in the movie.

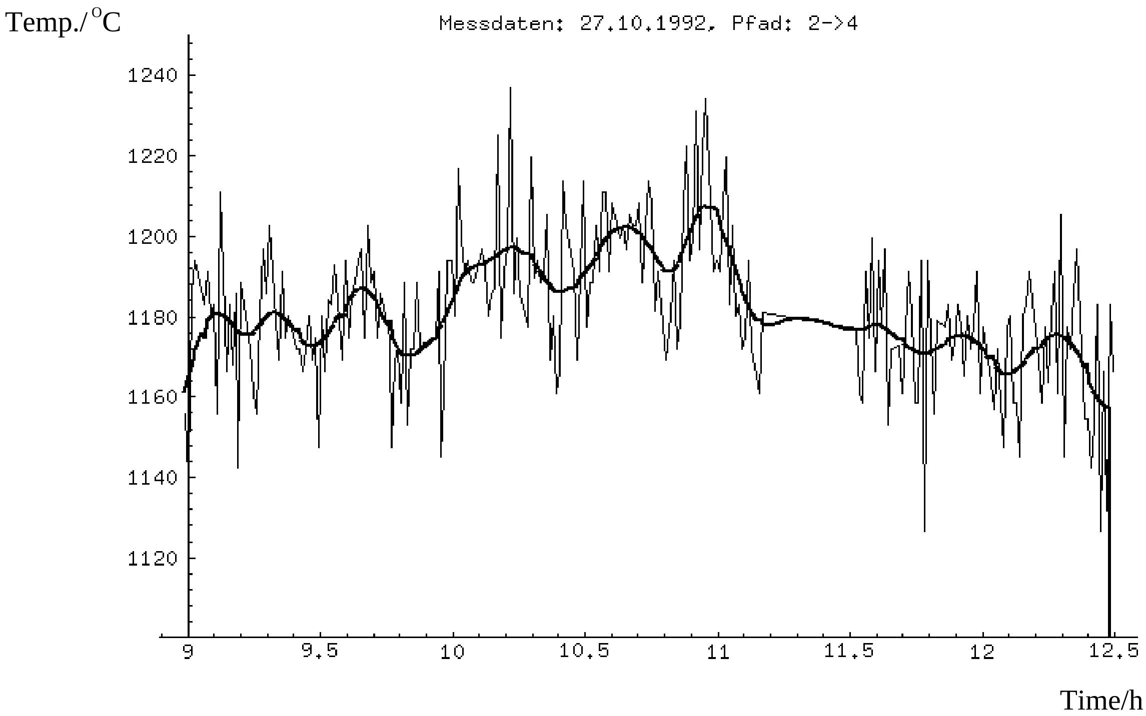

Fig 3: Approximation of data from one path in one direction using a cubic spline

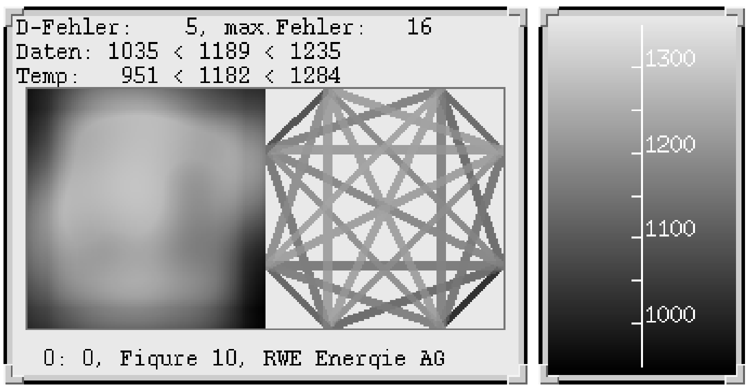

Fig 4: Reconstruction from measured data taken from [11]

REFERENCES

[1] W. Derichs, J. König: Die Schallpyrometrie — ein Meßverfahren zur Bestimmung der Temperaturverteilung in Kesselfeuerungen. DVV-Kolloquium, 1990.

[2] A. Trächtler: Use of Symmetries in Tomography. *Proc. European Concerted Action on Process Tomography*, Karlsruhe, 25-27 March 1993.

[3] A. Schwarz: Three-Dimensional Reconstruction of Temperature and Velocity Fields in a Furnace. *Proc. European Concerted Action on Process Tomography*, Oporto, 24-26 March 1994.

[4] F. Natterer: The Mathematics of Computerized Tomography. B. G. Teubner, 1986.

[5] E. Salerno, A. Tonazzini: 2D image reconstruction from sparse line-integral data. *Signal processing* **23** (1991) 193-203.

[6] H. Sielschott: Tomographie mit wenigen Daten: Anwendung von Kollokationsverfahren in der Schallpyrometrie. Abschlußbericht. Münster, June 1994.

[7] A. Lewitt: Alternatives to voxels for image representation in iterative reconstruction algorithms. *Phys. Med. Biol.*, 1992, Vol. 37, No 3, 705-716.

[8] B. Setzepfandt: ESNM: Ein rauschunterdrückendes EM-Verfahren für die Emissionstomographie. Thesis. Münster, July 1992.

[9] D. C. Youla, H. Webb: Image Restoration by the Method of Convex Projections: Part I — Theory. *IEEE Transactions on Medical Imaging*, Vol. MI-1, No. 2, October 1982.

[10] M. I. Sezan, H. Stark: Image Restoration by the Method of Convex Projections: Part 2 — Applications and Numerical Results. *IEEE Transactions on Medical Imaging*, Vol. MI-1, No. 2, October 1982.

[11] W. Derichs, F. Heß, K. Menzel, E. Reinartz: Acoustic Pyrometry: A correlation between temperature distributions and the operating conditions in a brown coal fired boiler. 2^{nd} International Conference On Combustion Technologies For A Clean Environment. Lissabon, July 1993.